AIP | The Journal of Chemical Physics

Can nonadditive dispersion forces explain chain formation of nanoparticles?

Bas W. Kwaadgras, Maarten W. J. Verdult, Marjolein Dijkstra, and René van Roij

Citation: J. Chem. Phys. **138**, 104308 (2013); doi: 10.1063/1.4792137
View online: http://dx.doi.org/10.1063/1.4792137
View Table of Contents: http://jcp.aip.org/resource/1/JCPSA6/v138/i10
Published by the American Institute of Physics.

Can nonadditive dispersion forces explain chain formation of nanoparticles?

Bas W. Kwaadgras,[1] Maarten W. J. Verdult,[2] Marjolein Dijkstra,[1] and René van Roij[2]
[1]*Debye Institute for Nanomaterials Science, Utrecht University, Princetonplein 5, 3584 CC Utrecht, The Netherlands*
[2]*Institute for Theoretical Physics, Utrecht University, Leuvenlaan 4, 3584 CE Utrecht, The Netherlands*

(Received 16 November 2012; accepted 29 January 2013; published online 11 March 2013)

We study to what extent dielectric nanoparticles prefer to self-assemble into linear chains or into more compact structures. To calculate the Van der Waals (VdW) attraction between the clusters we use the Coupled Dipole Method (CDM), which treats each atom in the nanoparticle as an inducible oscillating point dipole. The VdW attraction then results from the full many-body interactions between the dipoles. For non-capped nanoparticles, we calculate in which configuration the VdW attraction is maximal. We find that in virtually all cases we studied, many-body effects only result in local potential minima at the linear configuration, as opposed to global ones, and that these metastable minima are in most cases rather shallow compared to the thermal energy. In this work, we also compare the CDM results with those from Hamaker-de Boer and Axilrod-Teller theory to investigate the influence of the many-body effects and the accuracy of these two approximate methods. [http://dx.doi.org/10.1063/1.4792137]

I. INTRODUCTION

In recent years, the self-assembly of colloidal nanoparticles has received a large amount of attention. Many procedures have been proposed to achieve the desired highly ordered structures, e.g., by using systems with substrates or templates,[1] applying external electric, or magnetic fields[2–6] to particles with anisotropic response to these fields, or by using a fluid flow[7] to align the particles. One of the most widely used techniques, however, is the design and manipulation of particle-particle interactions, which can result in spontaneous self-assembly. Since the synthesis of anisotropically shaped particles has improved significantly in the past decade,[8,9] it is possible to control the shape of the particles and rely on excluded-volume interactions (possibly with the use of a depletant) to achieve alignment.[10,11] Alternatively, interaction design by controlling the relevant chemistry has also been successfully employed, for example in the form of patchy colloids,[12–14] or by the use of single-stranded DNA molecules as linkers.[15,16]

Spontaneous self-assembly of nanoparticles into linear chains has been observed experimentally. Various types of particles display this behavior. Observed systems include gold,[17] PbSe,[18–20] CdSe,[18,21–23] ZnSe,[23] and CdTe[24,25] nanoparticles. In the referenced papers, the behavior is attributed to the presence of a permanent dipole moment in the nanoparticles, although its origin is not entirely understood. Initial explanations attributed it to the intrinsic polar character of the wurtzite (CdSe) structure,[21] but this does not explain why the same behavior is observed in the nanoparticles of other structures. Other suggested origins include the presence of trapped, surface-localized charges,[23] and breaking of the nanoparticle's central symmetry due to asymmetric arrangement of crystal facets.[19]

More recent experimental[26,27] as well as theoretical and simulational[27] studies suggest that the capping layer plays an important role in the self-assembly of particles into various structures, including chains. The underlying mechanism here is a competition of the attractions between the particle cores with the entropy loss from distorting the capping layer polymer chains when two or more particles are close together. The linear conformation of the chains is explained by migration of ligands when two particles attach, making the site diametrically opposite the first contact point the most attractive for attachment of a third particle.[27] A detailed simulation study of the influence of the type of capping layer on two- and three-body interactions between nanoparticles[28] indeed suggests, among other things, that, due to the influence of the capping layer, a linear configuration of particles is energetically preferred over a triangular structure. These studies thus provide a possible explanation for spontaneous chain formation that does not depend on the presence of a permanent dipole. In this work, we investigate a third option, namely, the presence of nonpermanent, induced, fluctuating dipoles. These fluctuating dipoles are the origin of the Van der Waals (VdW) force between atoms and colloidal particles. This force is isotropic between two interacting atoms, but becomes orientation-dependent when more atoms are considered, since the fluctuating dipoles, like permanent ones, prefer to lie head-to-toe as opposed to side-by-side. Thus, to investigate this effect, we cannot rely on pairwise interactions between atoms, but have to calculate the full, many-atom VdW interaction, using a method called the Coupled Dipole Method (CDM), on which we elaborate in the next paragraph and Sec. II. It turns out that in virtually all cases we studied, many-body effects only result in local potential minima at the linear configuration, whereas the global minimum occurs for compact clusters. Moreover, these metastable minima are usually

rather shallow compared to the thermal energy. In most cases, the answer to the question asked in this Paper's title therefore seems to be "No." There are, however, extreme parameter regimes where linear configurations have the lowest energy.

The CDM, which models atoms as interacting inducible dipoles, was first introduced by Renne and Nijboer[29–31] in the 1960s. The method employs large-matrix manipulation to calculate the eigenmodes of the system under study; the sum of these frequencies then yields the ground state energy. The CDM takes many-body effects into account and can, therefore, be expected to be more accurate than both Hamaker-de Boer (HdB) theory,[32,33] which employs pairwise summation of atom-atom interactions, and a modification thereof, offered by Axilrod and Teller,[34] which includes three-atom interactions. In this work, we will examine the accuracy of the latter two methods, when compared to the CDM (which we will assume to be the "exact" result), for several many-atom systems.

At the time the CDM was conceived of, it was infeasible to perform the large-scale numerical calculations associated with the matrix manipulation, but computers of today can easily handle systems of at least $\mathcal{O}(10^4)$ atoms. Recently, the CDM has been employed to calculate interactions between, and also the polarizability of, nanoclusters of various sizes and shapes.[35–41] Furthermore, the accuracy of the first-, second- and third-order approximations of the CDM have been compared to the CDM itself in the context of graphitic nanostructures, yielding similar results to ours.[40]

For reasons that will be explained shortly, the CDM is only valid for non-metallic particles made of a material that satisfies $a_0/\alpha_0^{1/3} \gtrsim 1.7$, where a_0 is the lattice constant and α_0 the atomic polarizability associated with the material. Furthermore, all the calculations in this work are performed for particles in vacuum. To obtain results for particles in a medium, the atomic polarizability would have to be modified to a value that can be obtained by inserting the permittivity contrast between the particle and the medium into the Clausius-Mossotti relation.

II. METHODS

A. Atomic point dipoles

Throughout this paper, we will use the Lorentz-Drude model, which regards an atom as a nucleus of positive charge, with electrons harmonically bound to it. In this work, we consider only one electron (per nucleus) with charge $-e$ and, hence, a nucleus charge of $+e$. The polarization $\mathbf{p}$ of the atom is then simply given by $\mathbf{p} = e\mathbf{u}$, where $\mathbf{u}$ is the distance between the nucleus and the electron. Upon applying an external electric field $\mathbf{E}$, it can be shown that

$$\mathbf{p} = \alpha_0 \mathbf{E},$$

where (in CGS units)

$$\alpha_0 = \frac{e^2}{m_e \omega_0^2} \tag{1}$$

is the atomic polarizability. Here, m_e is the mass of the electron and ω_0 is the frequency associated with the harmonic force. In effect, an atom described in this way is a harmonic oscillator with frequency ω_0, therefore sometimes called a Drude oscillator.

Since in this model, the electrons are assumed to be bound to their nuclei, it does not apply to metals, because these contain unbound (free) electrons.

B. The coupled dipole method

The interaction between a pair of these atoms, at positions $\mathbf{r}_i$ and $\mathbf{r}_j$, is assumed to be the dipole-dipole interaction potential $-e^2 \mathbf{u}_i \cdot \mathbf{T}(\mathbf{r}_{ij}) \cdot \mathbf{u}_j$, where $\mathbf{u}_i$ is the distance vector between the nucleus and electron of atom i, and where we introduced a 3×3 dipole tensor

$$\mathbf{T}(\mathbf{r}_{ij}) \equiv \mathbf{T}_{ij} = \begin{cases} \left(3\mathbf{r}_{ij}\mathbf{r}_{ij}/r_{ij}^2 - \mathbf{I}\right)/r_{ij}^3 & \text{if } i \neq j, \\ \mathbf{0} & \text{if } i = j, \end{cases}$$

with $\mathbf{r}_{ij} = \mathbf{r}_i - \mathbf{r}_j$ and $r_{ij} = |\mathbf{r}_{ij}|$. In the case of N atoms in vacuum, all at fixed positions, we can write the Hamiltonian as a set of coupled harmonic oscillators

$$H = \frac{1}{2m_e} \sum_{i=1}^{N} \mathbf{k}_i^2 + \frac{m_e \omega_0^2}{2} \sum_{i,j=1}^{N} \mathbf{u}_i (\mathbf{I}\delta_{ij} - \alpha_0 \mathbf{T}_{ij}) \cdot \mathbf{u}_j, \tag{2}$$

where we used $\mathbf{k}_i$ to denote the linear momentum of the ith electron. The Hamiltonian of Eq. (2) represents a set of coupled harmonic oscillators. The angular eigenfrequencies of this system, ω_k with $k = 1, 2, \ldots, 3N$, depend solely on the dimensionless positions $\mathbf{r}_i/\alpha_0^{1/3}$ of the dipoles and on ω_0 (or, equivalently via Eq. (1), α_0). For $N \lesssim 10^4$ it is numerically fairly straightforward to find these eigenfrequencies, and hence the quantum mechanical ground state energy[29–31,35–39]

$$E\left(\left\{\mathbf{r}_i/\alpha_0^{1/3}\right\}; \omega_0\right) = \frac{\hbar}{2} \sum_{k=1}^{3N} \omega_k, \tag{3}$$

where $\hbar$ is the reduced Planck constant.

In this paper, we are interested in the effective interactions between nanoparticles composed of atomic dipoles. These nanoparticles are described as clusters of atomic dipoles arranged in a cubic lattice with lattice spacing a_0 such that they form a cubic or an (approximately) spherical nanoparticle. We will only consider interactions between identical nanoparticles. If we assign each nanoparticle a center-of-mass-position $\mathbf{R}_i$, the spectrum of eigenfrequencies ω_k only depends on the atomic eigenfrequency ω_0, the number of atoms in each nanoparticle, the dimensionless combinations $\mathbf{R}_{ij}/a_0$, where $\mathbf{R}_{ij} = \mathbf{R}_i - \mathbf{R}_j$, and the dimensionless lattice spacing

$$a \equiv a_0/\alpha_0^{1/3}.$$

Typical values of a are, in vacuum, $a = 2.64$ for hexane, $a = 2.05$ for silica and $a = 1.75$ for sapphire.[38] For low values of a, we encounter a polarization catastrophe, where the interactions become so strong that they overcome the harmonic binding force between the nuclei and their electrons, and the material becomes ferromagnetic. In the CDM, the catastrophe manifests itself by some of the frequencies ω_k becoming imaginary. For large numbers of atoms, the value at which the

catastrophe occurs lies between $a \approx 1.70$ and $a \approx 1.75$, depending on the lattice type. For very low numbers of atoms, the interatomic distance is allowed to be somewhat smaller; e.g., in Sec. III A, we show a setup with three atoms where the CDM is valid for $a \gtrsim 1.44$.

To obtain the effective interaction energy $V_2^{(CDM)}(\mathbf{R}_1, \mathbf{R}_2)$ between two nanoparticles at position $\mathbf{R}_1$ and $\mathbf{R}_2$ we subtract the ground state energy at infinite separation, which is the same as the energy of each nanoparticle if the other were absent

$$\begin{aligned} V_2^{(CDM)}(\mathbf{R}_1, \mathbf{R}_2) &= E_2^{(CDM)}(\mathbf{R}_1, \mathbf{R}_2) - E_1^{(CDM)}(\mathbf{R}_1) \\ &\quad - E_1^{(CDM)}(\mathbf{R}_2) \\ &= E_2^{(CDM)}(\mathbf{R}_1 - \mathbf{R}_2) - 2E_1^{(CDM)}. \end{aligned} \quad (4)$$

Here, $E_2^{(CDM)}(\mathbf{R}_1, \mathbf{R}_2)$ is the CDM-energy of the system by taking the positions of the atoms in the clusters at $\mathbf{R}_1$ and $\mathbf{R}_2$ and plugging them into Eq. (3), and $E_1^{(CDM)}(\mathbf{R}_i)$ is obtained by plugging only the positions of the atoms in cluster i into Eq. (3). In the second line, we have resolved some of the dependencies by noting that, in the case of two clusters, translational symmetry requires that $E_2^{(CDM)}(\mathbf{R}_1, \mathbf{R}_2) = E_2^{(CDM)}(\mathbf{R}_1 - \mathbf{R}_2)$ only depends on the relative cluster coordinates, and that $E_1^{(CDM)}(\mathbf{R}_i) = E_1^{(CDM)}$ does not depend on the center-of-mass position of the particle. Note that in this simplification, we also use that the clusters are identical.

If the system consists of two "clusters" consisting each of only one atom with polarizability α_0, separated by a distance r, calculation of the interaction is possible analytically within the CDM. When we Taylor-expand the result up to quadratic order for large interatomic distance, we find that the r^0 and r^{-3} terms of the expansion vanish and that we are left with only an r^{-6} term

$$V_2^{(CDM)}(r) \simeq -\frac{3}{4}\hbar\omega_0 \frac{\alpha_0^2}{r^6} \quad \left(r \gg \alpha_0^{1/3}\right). \quad (5)$$

This is the VdW interaction energy between two atoms.

For three clusters, the effective interaction energy is the sum of the effective interaction energies $V_2^{(CDM)}(\mathbf{R}_i, \mathbf{R}_j)$, plus the three-body term

$$\begin{aligned} &V_3^{(CDM)}(\mathbf{R}_1, \mathbf{R}_2, \mathbf{R}_3) \\ &\quad = E_3^{(CDM)}(\mathbf{R}_1, \mathbf{R}_2, \mathbf{R}_3) - V_2^{(CDM)}(\mathbf{R}_1, \mathbf{R}_2) \\ &\quad\quad - V_2^{(CDM)}(\mathbf{R}_2, \mathbf{R}_3) - V_2^{(CDM)}(\mathbf{R}_1, \mathbf{R}_3) \\ &\quad\quad - E_1^{(CDM)}(\mathbf{R}_1) - E_1^{(CDM)}(\mathbf{R}_2) - E_1^{(CDM)}(\mathbf{R}_3) \\ &\quad = E_3^{(CDM)}(\mathbf{R}_1, \mathbf{R}_2, \mathbf{R}_3) - E_2^{(CDM)}(\mathbf{R}_1 - \mathbf{R}_2) \\ &\quad\quad - E_2^{(CDM)}(\mathbf{R}_2 - \mathbf{R}_3) - E_2^{(CDM)}(\mathbf{R}_1 - \mathbf{R}_3) \\ &\quad\quad + 3E_1^{(CDM)}. \end{aligned} \quad (6)$$

Here, $E_3^{(CDM)}(\mathbf{R}_1, \mathbf{R}_2, \mathbf{R}_3)$ is obtained by plugging the atom positions of all three clusters into Eq. (3), and the second equality is obtained by using Eq. (4) and resolving the dependencies, as in the two-body case.

C. The Hamaker-de Boer potential

A widely used method for calculating the interaction energy in a colloidal system is by summation of the London potential between pairs of fluctuating dipoles. Given a set of atoms with locations $\{\mathbf{r}_i\}$ (where $i = 1, \ldots, N$), the total HdB interaction energy is given by

$$E^{(HdB)}(\{\mathbf{r}_i\}) = \sum_{(ij)} v^{(L)}(r_{ij}), \quad (7)$$

where $v^{(L)}(r_{ij})$ is the London interaction between atom i and j, given by

$$v^{(L)}(r) = -\frac{A}{r^6}, \quad (8)$$

where A is a constant determined by the two atoms' ionization energies and where r is the distance between the atoms. When dealing with clusters of atoms, $E^{(HdB)}(\{\mathbf{r}_i\})$ will not only contain interactions between pairs of atoms in different clusters, but also between pairs of atoms in the same cluster. Since we are only interested in the interaction energy between the clusters, we subtract the latter from their total energy to obtain the HdB inter-cluster interaction energy $V_2^{(HdB)}(\mathbf{R}_1, \mathbf{R}_2)$. For two clusters located at $\mathbf{R}_1$ and $\mathbf{R}_2$, respectively, we have, similar to Eq. (4),

$$\begin{aligned} V_2^{(HdB)}(\mathbf{R}_1, \mathbf{R}_2) &= E_2^{(HdB)}(\mathbf{R}_1, \mathbf{R}_2) - E_1^{(HdB)}(\mathbf{R}_1) \\ &\quad - E_2^{(HdB)}(\mathbf{R}_2) \\ &= E_2^{(HdB)}(\mathbf{R}_1 - \mathbf{R}_2) - 2E_1^{(HdB)}. \end{aligned}$$

Here, $E_2^{(HdB)}(\mathbf{R}_1, \mathbf{R}_2)$ is obtained by considering the atoms of both clusters 1 and 2 for Eq. (7), while $E_1^{(HdB)}(\mathbf{R}_i)$ is obtained by only considering the atoms of cluster i. For three clusters, it turns out that $V_3^{(HdB)}$ (defined similar to $V_3^{(CDM)}$) vanishes because only atomic pair interactions are considered.

The constant A to be used in Eq. (8) can be calculated in various ways. In this work, we intend to compare the HdB method to the CDM, and we therefore require that the long-range interaction energy between two atoms be equal when calculated using Eq. (8) and when using CDM (Eq. (5)). Comparing Eq. (5) with Eq. (8), we find

$$A = \frac{3}{4}\hbar\omega_0\alpha_0^2. \quad (9)$$

This is in agreement with, for example, the results in Ref. 42, Eq. (5), if $u_1 = \hbar\omega_0$ is inserted into that equation. Note that $\hbar\omega_0$ is the energy cost of ionizing the harmonic (Drude) oscillator, as expected.

D. The Axilrod-Teller potential

The HdB potential only includes pair interactions and ignores any many-body interactions. In 1943, Axilrod and Teller[34] approximated the three-body contribution to the atomic interaction energy,

$$v^{(AT)}(r_i, r_j, r_k) = B\frac{1 + 3\cos\theta_i \cos\theta_j \cos\theta_k}{r_{ij}^3 r_{jk}^3 r_{ki}^3}, \quad (10)$$

where $\cos\theta_i = \hat{\mathbf{r}}_{ij} \cdot \hat{\mathbf{r}}_{ik}$, and B is, according to Ref. 42 with $u_1 = \hbar\omega_0$, given by

$$B = \frac{9}{16}\hbar\omega_0\alpha_0^3.$$

We note that Eq. (10), such as Eq. (8), is a good approximation only for sufficiently large distances. The total Axilrod-Teller (AT) potential energy is the HdB potential energy, extended by a summation over dipole triplets,

$$E^{(AT)}(\{\mathbf{r}_i\}) = E^{(HdB)}(\{\mathbf{r}_i\}) + \sum_{(ijk)} v^{(AT)}(r_i, r_j, r_k), \qquad (11)$$

and the interaction energy between clusters of dipoles can be defined in the usual way, i.e., by Eqs. (4) and (6), where the superscript (*CDM*) is replaced by (*AT*), and $E_1^{(AT)}$, $E_2^{(AT)}(\mathbf{R}_i, \mathbf{R}_j)$ and $E_3^{(AT)}(\mathbf{R}_i, \mathbf{R}_j, \mathbf{R}_k)$ are now calculated using Eq. (11).

As far as we are aware, there is no closed expression for the CDM potential energy of three dipoles in an arbitrary configuration and therefore, it is in general not possible to compare the expression of the AT potential energy to that of the Taylor expansion of the CDM potential energy, as we did in the case of two dipoles. However, for the special case of an atomic triplet where $r_{12} = r_{23}$, we show in the Appendix that the AT potential equals the first two nonzero terms of this Taylor expansion of the CDM potential energy.

E. A note on notation

In this paper, we only consider setups where a number of clusters (usually two) are stationary, while an extra cluster is moved. For computational simplicity we will therefore consider the stationary clusters as one, so that we only calculate $V_2^{(CDM)}$, $V_2^{(HdB)}$, and $V_2^{(AT)}$ between the moving and the stationary clusters. In the case of three clusters, we have also analyzed the system when considered as three independent clusters, and calculated $V_3^{(CDM,HdB,AT)}$ plus the three cluster pair interactions $V_2^{(CDM,HdB,AT)}$. As expected, the resulting interaction energy plots are the same, albeit shifted by a constant. Since every interaction energy we calculate in this paper is a $V_2^{(CDM,HdB,AT)}$, we can ease the notation: from now on, we denote the interaction energy of the moving cluster with respect to the stationary ones by V_{CDM}, V_{HdB}, and V_{AT}.

III. CHAINS VERSUS COMPACT CLUSTERS

A. Atomic chains and clusters

Before discussing nanoparticles each composed of many atoms, we first consider N single atoms fixed on a straight line, separated by a lattice constant a_0. We consider an $N+1$th atom near the end of the chain, such that the vector separating this atom from the last atom in the chain has length a_0 and makes an angle θ with the line. This is illustrated in Fig. 1 for $N = 2$ (note that $r = a_0$ in the case of single dipoles). We calculate the CDM, HdB and AT interaction energies $V_{CDM}(\theta)$, $V_{HdB}(\theta)$, and $V_{AT}(\theta)$, respectively, between the $N+1$th atom and the cluster formed by the N atoms on the line, as a function of the angle θ, to study the most favorable (lowest energy) position of the additional atom. Here θ varies from $\theta = 0$, corresponding to the linear configuration, to $\theta = 2\pi/3$, corresponding to an equilateral triangle of the three end-particles of the chain. It is not *a priori* clear which of these configurations is more stable: the orientational dependence of the dipole-dipole interaction favors a linear arrangement and hence $\theta = 0$, but the $1/r^3$ decay of dipolar interactions favors small distances between the particles and hence $\theta = 2\pi/3$. If $V(0) < V(2\pi/3)$, the linear chain is more stable, while otherwise, a dense globule is favored.

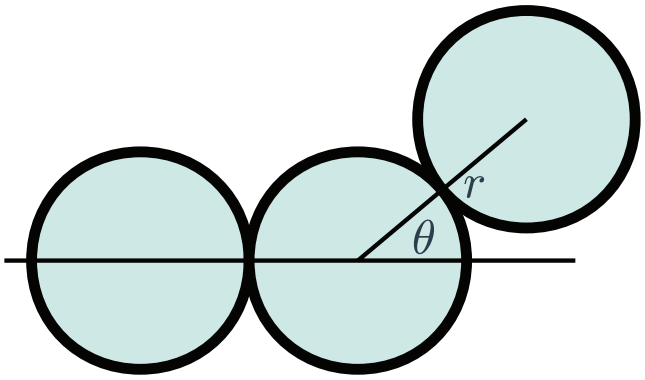

FIG. 1. The angle θ is defined as the angle between the line connecting the first two particles and the line connecting the last two particles. The distance between two successive particles is r. The situation here depicted is for $N = 2$.

In Fig. 2, we plot $V_{CDM}(\theta)$, $V_{HdB}(\theta)$, and $V_{AT}(\theta)$ for $N = 2$, 3, and 10, with $\alpha_0 = 5.25$ Å (such that $\omega_0 = \sqrt{\frac{e^2}{m_e\alpha_0}} = 6.9 \times 10^{15} s^{-1}$) for the dimensionless lattice spacings $a = 2.0$ and $a = 1.7$, the latter corresponding to stronger coupling. Note that we represent the interaction energies in units of k_BT, with k_B the Boltzmann constant and $T = 293$ K.

Concentrating first on V_{CDM} (solid lines) only, we note that for both $a = 2.0$ and $a = 1.7$, the configuration where the final three particles form an equilateral triangle is stable, by typically $1.5k_BT$ for $a = 2.0$ and by $4k_BT$ for $a = 1.7$. However, the insets also clearly show that for all cases a broad local minimum at $\theta = 0$ is separated from the global minimum at $\theta = 2\pi/3$ by a maximum at $\theta \approx 0.32\pi$ for $a = 2.0$ and at $\theta \approx 0.42\pi$ for $a = 1.7$. The barrier between the local and global minimum depends on the coupling parameter a: it is much smaller than k_BT in the weak coupling case of $a = 2.0$, while it grows to almost $1k_BT$ for $N = 10$ and $a = 1.7$. Hence, in both cases we expect thermal fluctuations to allow for relatively fast crossing of this barrier, such that the linear configurations should be short-lived at best.

When comparing the results of the CDM to those of the HdB and AT methods, there are several things to note. First of all, the accuracy of the approximation is dependent on the interatomic distance: at weaker coupling, $a = 2.0$, they are much more accurate than at stronger coupling, $a = 1.7$. We note, furthermore, that the accuracy is also dependent on θ, higher values of which (more compact clusters) tend to produce a slightly better agreement. Comparing the HdB and the AT, we note first of all, that AT seems to approximate the features of the CDM graph better than the HdB method, exhibiting a local minimum at $\theta = 0$, a barrier at $\theta \approx 0.3\pi$, and a

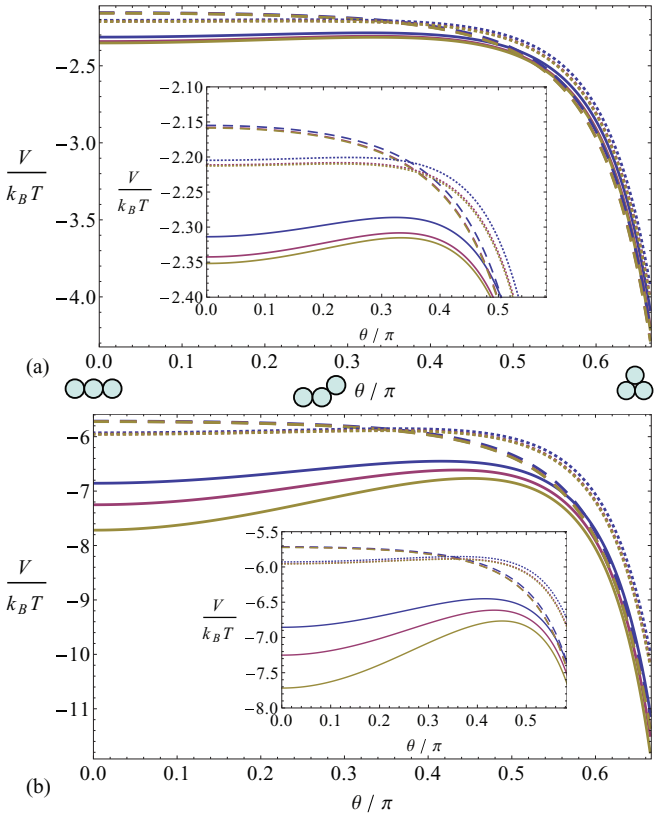

FIG. 2. Angular dependence of the interaction potential $V(\theta)/k_BT$, where $T = 293$ K, of adding a particle to the end of a string of N particles at $r = a_0$ (see Fig. 1), for dimensionless lattice constant $a = 2.0$ (a) and $a = 1.7$ (b), and for $N = 2$ (blue), $N = 3$ (red), and $N = 10$ (yellow). The results of three calculation methods are shown: the Coupled Dipole Method (solid lines), the Hamaker-de Boer method (dashed lines), and the Axilrod-Teller method (dotted lines). The inset shows a magnification of the small-angle part of $V(\theta)$.

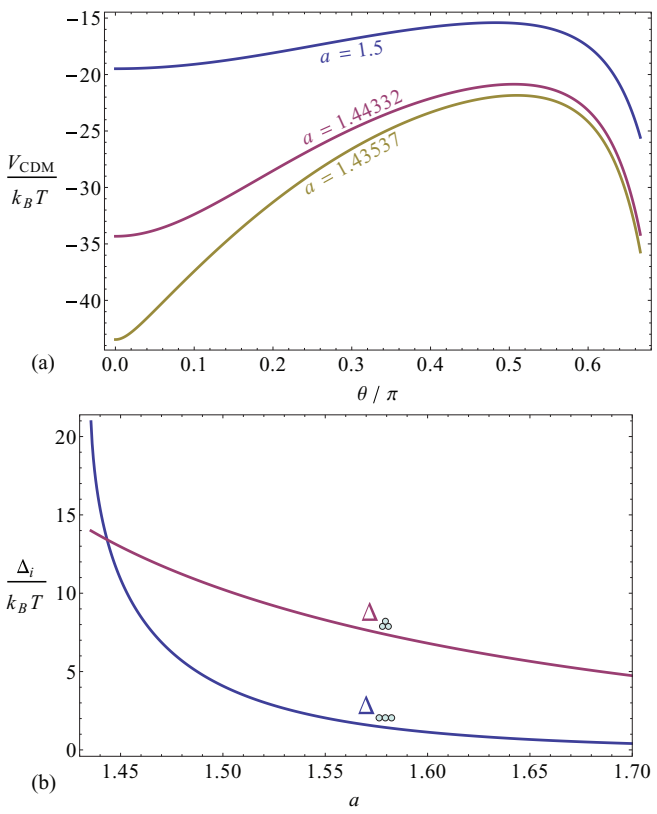

FIG. 3. (a) The CDM interaction energy V_{CDM}, in room temperature ($T = 293$ K) k_BT units, of adding a third dipole with polarizability $\alpha_0 = 5.25$ Å^3 to a chain of two, under an angle θ (defined in Fig. 1). The dimensionless dipole-dipole distance is $a = r/\alpha_0^{1/3} = 1.50$ (blue line), 1.44332 (red line), and 1.43573 (yellow line). (b) The well depth, defined as the difference in interaction energy at the well's configuration and the maximal interaction energy (here located at around $\theta \approx 0.5\pi$), of the linear ($\theta = 0$) configuration (blue) and the triangular ($\theta = 2\pi/3$) configuration (red).

global minimum at $\theta = 2\pi/3$, whereas the HdB method yields a monotonically decreasing function with its minimum at $\theta = 2\pi/3$. In passing, we can therefore note that many-body effects are clearly responsible for creating a local minimum at the linear configuration. In terms of absolute numbers, the accuracy depends on θ: AT produces better results for low angles, while the HdB method actually beats AT for high angles. Both HdB and AT underestimate the effect of adding a dipole to the chain: the graphs for the various values of N are very close together for HdB and AT, while the CDM produces clearly separated graphs.

From a theoretical perspective, it is interesting to investigate the behavior of $V_{CDM}(\theta)$ for values of a that are lower (i.e., stronger coupling) than the aforementioned value of 1.7. For (large) lattices of atoms, the CDM fails for such low a, since some of the eigenfrequencies ω_k become imaginary. In the specific case of three dipoles forming a configuration as in Fig. 1, however, the lower limit is $a \approx 1.435194$. In Fig. 3(a), we show what happens to $V_{CDM}(\theta)$ when a is lowered to this value. The HdB and AT approximations, $V_{HdB}(\theta)$ and $V_{AT}(\theta)$, respectively, are not considered here, since for low a, they become increasingly inaccurate. We clearly see that both the potential well at $\theta = 2\pi/3$ (the triangular configuration) and the one at $\theta = 0$ (the linear configuration) deepen as a is lowered, but that the $\theta = 0$ well deepens more. Below the value $a \approx 1.44332$, the well at the linear configuration becomes the deeper of the two. We note that, when compared with the aforementioned lower limit, that makes the range of values for a for which a linear configuration is favorable extremely narrow. Note, however, that the barrier between the metastable and the stable configurations grows significantly with decreasing a, being approximately $4k_BT$ at $a = 1.5$ and $14k_BT$ at $a \approx 1.44$, which could cause long-lived linear triplets. This is also visible in Fig. 3(b), where the depths Δ of the wells at $\theta = 0$ and $\theta = 2\pi/3$ are plotted as a function of a.

It should be noted that throughout this subsection, we have varied the dimensionless dipole-dipole distance $a = a_0/\alpha_0^{1/3}$ by fixing α_0 and varying a_0. Another option is to fix a_0 and vary α_0 instead. This affects the results, because ω_k/ω_0 depends on a only, and hence the eigenfrequencies ω_k (and, thus, V_{CDM}) are proportional to $\omega_0 \propto \alpha_0^{-1/2}$. Therefore, the shape of the graphs in Fig. 3(b), where a is the variable, become different, and the relative height of the various graphs of V_{CDM} (Figs. 2(a), 2(b), and 3(a)) with different a change. However, as it turns out, these changes are not significant enough to warrant reporting here (for the parameters of interest), and the same qualitative conclusions apply.

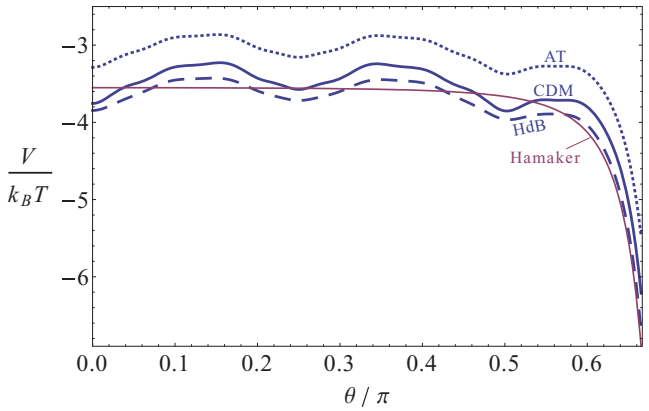

FIG. 4. Interaction potential for three spherical nanoclusters of radius $R = 3.85a_0$, giving 321 silica particles each, with dimensionless lattice spacing $a = 2.0$, as a function of the angle θ between the line connecting the first and second, and the one connecting the second and third cluster. The results of four calculation methods are shown: the Coupled Dipole Method (solid blue lines), the Hamaker-de Boer method (dashed blue lines), the Axilrod-Teller method (dotted blue lines), and the result from Hamaker's formula Eq. (12) (the solid red line).

B. Clusters and chains of spherical nanoclusters

We now focus on chains of spherical nanoparticles. We perform these calculations with spherical nanoparticles made from silica atoms ($\alpha_0 = 5.25$ Å), which are positioned on a face-centered cubic (fcc) lattice with $a = 2.0$. To create a single nanoparticle of radius R, we start by placing the silica atoms on the grid and then remove all of them located further than a distance R away from the origin. Hence, we obtain an approximately spherical cluster with radius R. Furthermore, we use the same definition for r and θ as given in Fig. 1 for the single particles. Now we fix $r = 2R + a_0$ and proceed in the same manner as above to calculate the interaction energy between a cluster consisting of two spheres and a third sphere as a function of the angle θ. It is again not *a priori* clear which is the more stable orientation: the orientational dependence of the dipole-dipole attraction will favor a linear arrangement ($\theta = 0$), whereas the $1/r^3$ decay will favor the small distances between the particles ($\theta = 2\pi/3$).

The resulting angle-dependence of the potential is, for $R = 3.85a_0$ ($N_c = 321$ particles in each cluster), given in Fig. 4 for CDM, HdB, and AT. Also shown is the result when we use Hamaker's famous expression for the interaction energy between a pair of spheres,[32]

$$V_{\text{Hamaker}}(r,\sigma) = -\frac{\pi^2\rho^2 A}{12}\left(\frac{\sigma^2}{r^2-\sigma^2}+\frac{\sigma^2}{r^2} + 2\log\left[\frac{r^2-\sigma^2}{r^2}\right]\right), \tag{12}$$

where σ is the diameter of the spheres, r is the center-to-center distance between the spheres (given above), A is the London-VdW constant, in our case given by Eq. (9), and ρ is the number density of atoms in the sphere, which can be obtained by noting that for a fcc lattice with $a_0/\alpha_0^{1/3} = 2$,

$$\rho = \frac{2}{\sqrt{2}a_0^3} = \frac{1}{4\sqrt{2}\alpha_0},$$

so that $\pi^2\rho^2 A \approx 42k_BT$ at room temperature. Since our clusters are not exactly spherical, and the outer atoms are never exactly a distance R away from the sphere center, the value to use for σ is nontrivial. We derive it by considering the dependence of the mean square displacement $\langle r'^2\rangle_{\text{ball}}$ of mass inside a solid sphere, with homogeneous mass density ρ, on its diameter d,

$$\langle r'^2\rangle_{\text{ball}} = \frac{\int d\mathbf{r}'\rho r'^2}{\int d\mathbf{r}'\rho} = \frac{4\pi\int_{r=0}^{d/2} dr' r'^4}{4\pi\int_{r=0}^{d/2} dr' r'^2} = \frac{3}{20}d^2,$$

where r' is the distance of a mass element $\rho d\mathbf{r}'$ from the center of the sphere. We now assume that the mean square displacement of atoms inside our spherical atom clusters, $\langle r_i^2\rangle_c = \frac{1}{N_c}\sum_{i=1}^{N_c} r_i^2$ where r_i is the distance of atom i from the center of the sphere, obeys the same relationship, $\langle r_i^2\rangle_c = \frac{3}{20}\sigma^2$, such that

$$\sigma = \sqrt{\frac{20}{3N_c}\sum_{i=1}^{N_c} r_i^2}.$$

The numerical value for our clusters with $R = 3.85a_0$ turns out to be

$$\sigma \approx 7.55a_0 \approx 0.98 \times 2R.$$

The results of the CDM, HdB, and AT methods are similar to those observed for the atomic chains above, i.e., there is a local minimum at $\theta = 0$, when all three nanoclusters line up, while the global minimum is in the triangle orientation ($\theta = 2\pi/3$). The difference between the local minimum at $\theta = 0$ and the global minimum at $\theta = 2\pi/3$ is of the order of $3k_BT$. The main difference with the atomic chain is the additional wells at $\theta \approx 0.25\pi$ and $\theta \approx 0.5\pi$, separated by barriers of the order of $0.5k_BT$. This structure is caused by the relatively small size of the spherical nanoclusters (only 321 particles each), which renders the surfaces of the clusters not very smooth, causing the edges of the particles to "coincidentally" be closer to each other for some values of θ than for others. Surprisingly, the AT approximation, in this case, gives worse results than the HdB approximation.

The graph obtained from $V_{\text{Hamaker}}(r,\sigma)$ is quite accurate in shape and displays a very good quantitative agreement with the HdB approximation. This is remarkable, because for values of σ so close to r, the effective interaction energy depends strongly on σ. The graph does not contain local minima, since in this method, the spheres are assumed to consist of a continuous, homogeneous material, and the atoms are not individually modeled.

C. Clusters and chains of cubic nanoclusters

Next, we consider $L \times L \times L$ cubic nanoparticles of $N_c = L^3$ atoms on a cubic lattice with lattice spacing a_0. Similar to the case above, we focus on a configuration of three particles: two lined up and close together, forming essentially a single $2L \times L \times L$ particle, with a third particle in its vicinity. We present results for clusters with $L = 5$. For the cubic particles of interest, we will use Cartesian coordinates instead of the polar coordinates used before, with the x-direction

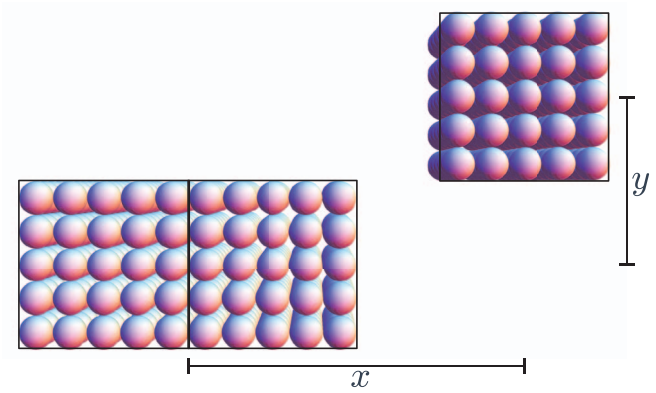

FIG. 5. Orientation of the system of interest for three cubic clusters of which two are lined up and the third is a distance (x, y) away.

parallel to the chain and y- and z-directions perpendicular, as illustrated in Fig. 5.

We consider here two cases, both for coupling constant $a = 2.0$. First, we vary y for fixed $x = 7.5a_0$, such that the third particle can (just) slide "vertically" past the other two on the right side. Note that this means that when $y = 0$, all three clusters lie on the same line and are touching (i.e., this corresponds to the $\theta = 0$ orientation of the spherical clusters). Second, we fix $y = 5a_0$ and vary x, such that the third particle slides "horizontally" along x on top of the other two particles.

The results are plotted in Fig. 6. Figure 6(a) shows the potential $V(x = 7.5a_0, y)$ for the first, "vertical" case, revealing local minima at (roughly) $y/a_0 \approx 0, \pm 0.96, \pm 1.93$, and ± 2.89, while a "pseudo-minimum" (inflection point) occurs at $y/a_0 \approx \pm 3.82$. These correspond to alignment of horizontal sheets of atoms in the three $5 \times 5 \times 5$ nanoclusters; we interpret the small deviation from perfect alignment (which occurs at $y/a_0 = 0, \pm 1, \pm 2$, etc.) as a finite-size effect. The global minimum in Fig. 6(a) occurs for the linear chain characterized by $y = 0$. The energy barriers between adjacent local minima vary from roughly $5.9k_BT$ between $y/a_0 = \pm 0.96$ and $y/a_0 = 0$, and $2.7k_BT$ from $y/a_0 = \pm 1.93$ to $y/a_0 = \pm 0.962$, to vanishingly small barriers for $y/a_0 \geq 3$. As a consequence, one could expect (temporary) trapping in local minima at $y/a_0 = \pm 0.96$ and ± 1.93. Figure 6(b) shows the potential $V(x, y = 5a_0)$ for the second, "horizontal" case. Again, we observe local minima, near where vertical sheets of atoms align, in this case for $x/a_0 \approx \pm 0.50, \pm 1.50, \pm 2.48, \pm 3.45, \pm 4.43, \pm 5.38$. The six deepest ones (with $|x/a_0| < 2.5$) are essentially degenerate and separated by barriers of about $15k_BT$. We note that the minima occur closer to perfect alignment when the third cube is near the middle: here, the effect of the edges of the first two cubes is smallest. For $|x/a_0| \gtrsim 7/2$, we can still make out the points where either 4, 3, 2, or 1 sheet(s) align(s).

Combining the information of Figs. 6(a) and 6(b) reveals that the global minimum, for these $5 \times 5 \times 5$ clusters, occurs in the vicinity of the "triangular" configuration, since $V(x = a_0/2, y = 5a_0) \approx -97k_BT$, whereas the deepest linear-chain minimum is $V(x = 7.5a_0, y = 0) = -91k_BT$, the difference being about $6k_BT$. One should realize, however, that the barrier(s) separating the two configurations are of the order of $100k_BT$, such that a chain, once formed, could exist

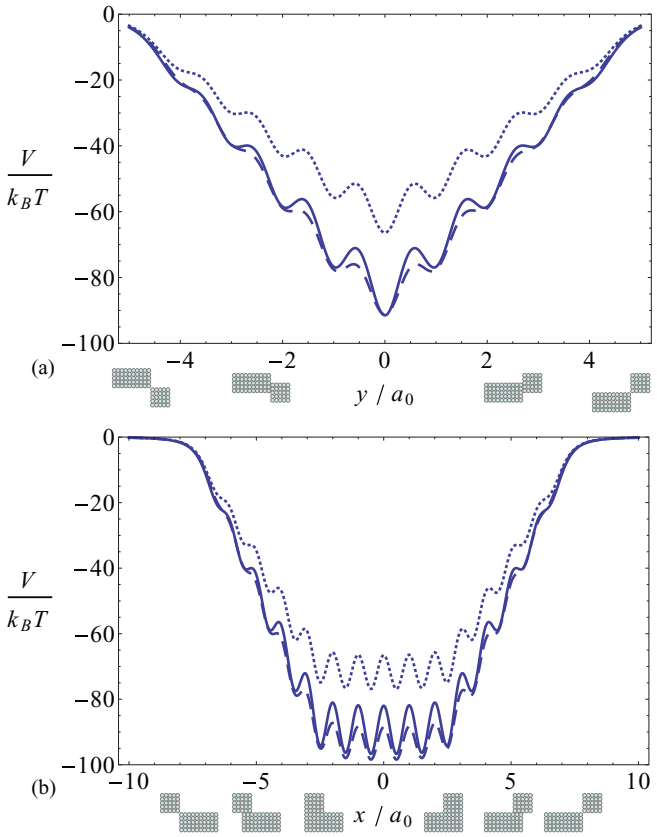

FIG. 6. Interaction potential for three cubic clusters of 125 particles each with lattice spacing $a_0 = 2.0\alpha_0^{1/3}$, (a) as function of the y-coordinate of the third cluster for fixed $x = 7.5a_0$ and (b) as function of the x-coordinate of the third cluster for fixed $y = 5a_0$. The results of three calculation methods are shown: the Coupled Dipole Method (solid lines), the Hamaker-de Boer method (dashed lines), and the Axilrod-Teller method (dotted lines).

essentially forever. It thus appears that the main difference between the attachment potential of atomic triplets (treated in an earlier section) and the $5 \times 5 \times 5$ triplets here is the existence of local minima separated by barriers due to the underlying atomic structure of the latter. These results are qualitatively similar to those of $3 \times 3 \times 3$ and $7 \times 7 \times 7$ particles.

We note again that the HdB approximation gives better results than the AT approximation, although the latter seems to better approximate the height of the inter-well barriers. We note that both the shape of the graphs, which feature local minima induced by the atomic structure, as well as the qualitative conclusion that HdB is more accurate than AT, are similar to those presented in Ref. 41. For this setup, we also calculated the net force on the third ("moving") particle by considering the gradient of V, but no interesting conclusions could be drawn from these calculations, except that the accuracy of the HdB and AT approximations remained roughly the same.

IV. SUMMARY AND CONCLUSION

In this work, we have addressed the question whether nonadditive dispersion forces can explain chain formation of nanoparticles. This we have done using the CDM, where we

model the nanoparticles as built up out of atoms and take into account all their many-body interactions. We have studied configurations of single atoms, spherical and cube-shaped atomic clusters. For almost all these systems, we have found a local minimum of the potential energy at the linear configuration, but a global minimum at the triangular one, making the latter thermodynamically favorable. For single dipoles the energy difference between the two configurations is generally several k_BT and the barrier between the two only of the order of, at most, one k_BT, such that we do not expect linear configurations to be stable. For a small parameter subspace we did find a stable linear configuration; however, given the small size of this region and the exotic parameters chosen, it seems unlikely that this has experimental significance. For spherical clusters of dipoles, we found only a stable triangular phase. For cubes, although the triangular configuration is the overall minimum, the energy barrier between the linear and triangular configuration is so large that, once formed, we expect either configuration to exist essentially forever.

In many of the studied cases, we have also investigated how accurate the HdB and AT methods of calculating the interaction energy are when compared to the result given by the CDM. From the studied cases, we can conclude that for strings of single dipoles, many-body effects are significant, especially when the coupling is strong. For the clusters consisting of many dipoles (i.e., spheres and cubes), we found that the HdB method performs very well and, in fact, much better than the AT method. A possible explanation for this is that, while both approaches are only exact when (dimensionless) dipole-dipole distances are large, the AT method might be more sensitive to dipoles being close together; and in a cluster of dipoles, each dipole has many nearby neighbors. More research is required to test this hypothesis. For spheres, we compared our results with Hamaker's expression which is obtained by integrating the Van der Waals interaction over the volume of two spheres.

In the work by Schapotschnikow *et al.*,[28] where simulation methods are used to arrive at an effective three-body interaction energy between triplets of nanoparticles stabilized by capping layers, it is suggested that linear chains are the overall most favorable orientation. In our work, we find that the CDM, which includes many-body VdW interactions between atoms but ignores steric interactions between the capping layers, shows that many-body linear chains are metastable, whereas the two-body HdB method exhibits no local minimum at the linear configuration. Still, in the CDM, the triangular configuration is overall more favorable, and the linear configuration is not stable enough to predict stable linear chains in a Brownian environment. From this, we can conclude, as already suggested by Schapotschnikow *et al.*,[28] that an important role in explaining chain formation could be played by effective three-body interactions between the particles' capping layers that make triangular configurations unfavorable. Many-atom VdW interactions, while not strong enough by themselves to make linear chains favorable, do provide a local minimum at this configuration, making it the most favorable configuration if triangular ones are excluded by steric interactions. This could provide an explanation for spontaneous chain formation that does not include permanent dipole moments. It would be of interest to include steric interactions in our calculations in the manner employed by Schapotschnikow *et al.*.[28] or, using the CDM, allowing for many-body interactions between ligand segments even during the simulation steps, thus calculating a full, many-body, effective, average interaction energy. This is left for future study.

ACKNOWLEDGMENTS

This work is part of the research programme of FOM, which is financially supported by NWO. Financial support by an NWO-VICI grant is acknowledged.

APPENDIX: ADDITIONAL MATHEMATICAL AND NUMERICAL COMPARISONS

For the atomic configuration described in Fig. 1 and Subsection III A, it is possible to calculate the CDM interaction energy exactly. The eigenfrequencies of the system are given by

$$\omega_k = \omega_0\sqrt{1+\lambda_k},$$

where the λ_k are the nine eigenvalues of a 9×9 matrix. These can be expressed in terms of the functions

$$\begin{aligned}
A_1(x) &= 1 + 512x^6 - 384x^8,\\
A_2(x) &= 192\sqrt{3}x^6(2-3x^2)^2,\\
B_1(x) &= 1 + 128x^6 + 384x^8,\\
B_2(x) &= 1728\sqrt{3}x^8(1-x^2),\\
f_1(x) &= \frac{\sqrt{A_1^{3/2}(x)+A_2(x)}}{\sqrt{A_1^{3/2}(x)-A_2(x)}},\\
f_2(x) &= \frac{\sqrt{B_1^{3/2}(x)+B_2(x)}}{\sqrt{B_1^{3/2}(x)-B_2(x)}}
\end{aligned}$$

and

$$\begin{aligned}
T_1(x) &= 3 + 2\sqrt{3A_1(x)}\cos\left[\frac{2}{3}\arctan(f_1(x))\right],\\
T_{2,3}(x) &= 3 - \sqrt{3A_1(x)}\left(\cos\left[\frac{2}{3}\arctan(f_1(x))\right]\right.\\
&\qquad \left.\pm\sqrt{3}\sin\left[\frac{2}{3}\arctan(f_1(x))\right]\right)\\
&= 3 - 2\sqrt{3A_1(x)}\cos\left[\frac{2}{3}\arctan(f_1(x)) \mp \frac{\pi}{3}\right],\\
T_4(x) &= -3 - 2\sqrt{3B_1(x)}\cos\left[\frac{2}{3}\arctan(f_2(x))\right],\\
T_{5,6}(x) &= -3 + \sqrt{3B_1(x)}\left(\cos\left[\frac{2}{3}\arctan(f_2(x))\right]\right.\\
&\qquad \left.\pm\sqrt{3}\sin\left[\frac{2}{3}\arctan(f_2(x))\right]\right)\\
&= -3 + 2\sqrt{3B_1(x)}\cos\left[\frac{2}{3}\arctan(f_2(x)) \mp \frac{\pi}{3}\right]
\end{aligned}$$

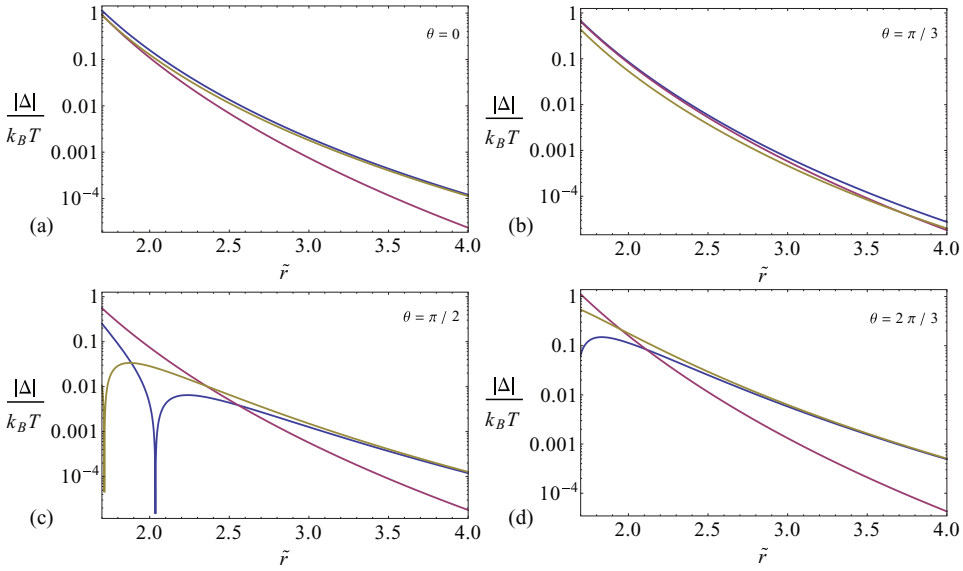

FIG. 7. The absolute difference $|\Delta|$ between V_{CDM} and V_{HdB} (blue), V_{CDM} and V_{AT} (red), and V_{CDM} and V_{cHdB} (yellow), corresponding, respectively, to Hamaker-de Boer, Axilrod-Teller, and "corrected HdB" (or, rather, Hamaker-de Boer but with unapproximated pair potentials) methods of approximation, for three dipoles positioned as in Fig. 1, as a function of the dimensionless distance $\tilde{r} = r/\alpha_0^{1/3}$ between the first two and the last two dipoles in the chain. We consider $\theta = 0$ (a), $\theta = \pi/3$ (b), $\theta = \pi/2$ (c), and $\theta = 2\pi/3$ (d).

by

$$\lambda_k(\tilde{r},\theta) = \frac{T_k\left(\cos\left[\frac{\theta}{2}\right]\right)}{24\tilde{r}^3\cos^3\left[\frac{\theta}{2}\right]} \quad (k = 1,\ldots,6),$$

$$\lambda_{7,8}(\tilde{r},\theta) = \frac{1 \pm \sqrt{1+512\cos^6\left[\frac{\theta}{2}\right]}}{16\tilde{r}^3\cos^3\left[\frac{\theta}{2}\right]},$$

$$\lambda_9(\tilde{r},\theta) = -\frac{1}{8\tilde{r}^3\cos^3\left[\frac{\theta}{2}\right]}.$$

Here, $\tilde{r}$ is the dimensionless distance $r/\alpha_0^{1/3}$. The total CDM interaction energy $V_{CDM}(\tilde{r},\theta)$ between the three dipoles is given by

$$V_{CDM}(\tilde{r},\theta) = \frac{1}{2}\hbar\omega_0\left[\sum_{k=1}^{9}\sqrt{1+\lambda_k} - 9\right].$$

This can be approximated for small λ_k (or, equivalently, large r) by a Taylor expansion of the square root

$$V_{CDM} \simeq \frac{1}{2}\hbar\omega_0\sum_{k=1}^{9}\left(\frac{1}{2}\lambda_k - \frac{1}{8}\lambda_k^2 + \frac{1}{16}\lambda_k^3\right).$$

It can be straightforwardly shown that $\sum_{k=1}^{9}\lambda_k = 0$, while it can also be (less straightforwardly) calculated that

$$\sum_{k=1}^{9}\lambda_k^2 = \frac{3}{16\tilde{r}^6\cos^6\left[\frac{\theta}{2}\right]} + \frac{24}{\tilde{r}^6},$$

$$\sum_{k=1}^{9}\lambda_k^3 = \frac{9\left(1+3\cos^2\left[\frac{\theta}{2}\right]-6\cos^4\left[\frac{\theta}{2}\right]\right)}{4\tilde{r}^9\cos^3\left[\frac{\theta}{2}\right]}.$$

It follows that

$$\frac{1}{2}\hbar\omega_0\sum_{k=1}^{9}\left(-\frac{1}{8}\lambda_k^2\right) = \sum_{(ij)}v^{(L)}(r_{ij}),$$

$$\frac{1}{2}\hbar\omega_0\sum_{k=1}^{9}\left(\frac{1}{16}\lambda_k^3\right) = v^{(AT)}(r_i,r_j,r_k),$$

as defined in Eqs. (8) and (11), thus confirming that in this case, the London and AT approximations follow from a Taylor expansion of the CDM result.

The accuracy of the HdB and AT approximations depends on the angle θ, but also greatly on the interatomic distance r. In Fig. 7, we illustrate this for the three-dipole case of Fig. 1 (Sec. III A), for a few values of θ, by plotting the absolute difference Δ between V_{CDM} and V_{HdB}, V_{CDM} and V_{AT}, and V_{CDM} and V_{cHdB}, where V_{cHdB} is the result obtained by only considering pair interactions in CDM but not Taylor-expanding the result in $\tilde{r}^{-3}$ (as is done for V_{HdB}). For large $\tilde{r}$, we observe that the AT approximation becomes the best of the three plotted methods; however, for smaller $\tilde{r}$, this is not always the case. The AT performs best for a straight line of dipoles ($\theta = 0$), but even here there is a region ($\tilde{r} \lesssim 1.8$) where it is beaten by V_{cHdB}. For $\theta = \pi/3$, V_{cHdB} outperforms V_{AT} up until $\tilde{r} \approx 3.75$. The straight-angled case ($\theta = \pi/2$) is interesting in that each of the three methods has a region where it has the best accuracy: V_{cHdB} for $\tilde{r} \lesssim 1.9$, V_L for $1.9 \lesssim \tilde{r} \lesssim 2.6$, and V_{AT} for $\tilde{r} \gtrsim 2.6$. In the case of the equilateral triangle ($\theta = 2\pi/3$), V_{HdB} beats V_{AT} in the region $\tilde{r} \lesssim 2.1$. We note that, with the exception of the straight-line case, AT only starts giving more accurate results than the other two methods in the regime $\tilde{r} > 2.1$, which was not considered in the main body of the present work.

[1]S. Ahmed and K. M. Ryan, Nano Lett. **7**, 2480 (2007).
[2]K. M. Ryan, A. Mastroianni, K. A. Stancil, H. Liu, and A. P. Alivisatos, Nano Lett. **6**, 1479 (2006).
[3]D. van der Beek, A. V. Petukhov, P. Davidson, J. Ferré, J. P. Jamet, H. H. Wensink, G. J. Vroege, W. Bras, and H. N. Lekkerkerker, Phys. Rev. E **73**, 041402 (2006).
[4]K. Bubke, H. Gnewuch, M. Hempstead, J. Hammer, and M. L. H. Green, Appl. Phys. Lett. **71**, 1906 (1997).
[5]A. F. Demirörs, P. M. Johnson, C. M. van Kats, A. van Blaaderen, and A. Imhof, Langmuir **26**, 14466 (2010).
[6]P. A. Smith, C. D. Nordquist, T. N. Jackson, T. S. Mayer, B. R. Martin, J. Mbindyo, and T. E. Mallouk, Appl. Phys. Lett. **77**, 1399 (2000).
[7]B. Sun and H. Sirringhaus, J. Am. Chem. Soc. **128**, 16231 (2006).
[8]S. C. Glotzer and M. J. Solomon, Nature Mater. **6**, 557 (2007).
[9]S.-M. Yang, S.-H. Kim, J.-M. Lima, and G.-R. Yi, J. Mater. Chem. **18**, 2177 (2008).
[10]L. Onsager, Ann. N.Y. Acad. Sci. **51**, 627 (1949).
[11]S. Sacanna, W. T. M. Irvine, P. M. Chaikin, and D. J. Pine, Nature (London) **464**, 575 (2010).
[12]G. Doppelbauer, E. Bianchi, and G. Kahl, J. Phys.: Condens. Matter **22**, 104105 (2010).
[13]F. Romano and F. Sciortino, Nature Mater. **10**, 171 (2011).
[14]Q. Chen, S. C. Bae, and S. Granick, Nature (London) **469**, 381 (2011).
[15]A. Travesset, Science **334**, 183 (2011).
[16]R. J. Macfarlane, B. Lee, M. R. Jones, N. Harris, G. C. Schatz, and C. A. Mirkin, Science **334**, 204 (2011).
[17]J. Liao, K. Chen, L. Xu, C. Ge, J. Wang, L. Huang, and N. Gu, Appl. Phys. A: Mater. Sci. Process. **76**, 541 (2003).
[18]M. Klokkenburg, A. J. Houtepen, R. Koole, J. W. J. de Folter, B. H. Erné, E. van Faassen, and D. Vanmaekelbergh, Nano Lett. **7**, 2931 (2007).
[19]K.-S. Cho, D. V. Talapin, W. Gaschler, and C. B. Murray, J. Am. Chem. Soc. **127**, 7140 (2005).
[20]A. J. Houtepen, R. Koole, D. Vanmaekelbergh, J. Meeldijk, and S. G. Hickey, J. Am. Chem. Soc. **128**, 6792 (2006).
[21]S. A. Blanton, R. L. Leheny, M. A. Hines, and P. Guyot-Sionnest, Phys. Rev. Lett. **79**, 865 (1997).
[22]L.-S. Li and A. P. Alivisatos, Phys. Rev. Lett. **90**, 097402 (2003).
[23]M. Shim and P. Guyot-Sionnest, J. Chem. Phys. **111**, 6955 (1999).
[24]Z. Tang, N. A. Kotov, and M. Giersig, Science **297**, 237 (2002).
[25]Z. Tang, Z. Zhang, Y. Wang, S. C. Glotzer, and N. A. Kotov, Science **314**, 274 (2006).
[26]M. S. Nikolic, C. Olsson, A. Salcher, A. Kornowski, A. Rank, R. Schubert, A. Frömsdorf, H. Weller, and S. Förster, Angew. Chem. Int. Ed. **48**, 2752 (2009).
[27]P. Akcora, H. Liu, S. K. Kumar, J. Moll, Y. Li, B. C. Benicewicz, L. S. Schadler, D. Acehan, A. Z. Panagiotopoulos, V. Pryamitsyn, V. Ganesan, J. Ilavsky, P. Thiyagarajan, R. H. Colby, and J. F. Douglas, Nature Mater. **8**, 354 (2009).
[28]P. Schapotschnikow and T. J. H. Vlugt, J. Chem. Phys. **131**, 124705 (2009).
[29]M. Renne and B. Nijboer, Chem. Phys. Lett. **1**, 317 (1967).
[30]B. Nijboer and M. Renne, Chem. Phys. Lett. **2**, 35 (1968).
[31]B. R. A. Nijboer and M. J. Renne, Phys. Norv. **5**, 243 (1971).
[32]H. Hamaker, Physica **4**, 1058 (1937).
[33]J. H. de Boer, Trans. Faraday Soc. **32**, 10 (1936).
[34]B. M. Axilrod and E. Teller, J. Chem. Phys. **11**, 299 (1943).
[35]H.-Y. Kim, J. O. Sofo, D. Velegol, M. W. Cole, and A. A. Lucas, J. Chem. Phys. **124**, 074504 (2006).
[36]H.-Y. Kim, J. O. Sofo, D. Velegol, M. W. Cole, and A. A. Lucas, Langmuir **23**, 1735 (2007).
[37]M. W. Cole and D. Velegol, Mol. Phys. **106**, 1587 (2008).
[38]H.-Y. Kim, J. O. Sofo, D. Velegol, M. W. Cole, and G. Mukhopadhyay, Phys. Rev. A **72**, 053201 (2005).
[39]B. W. Kwaadgras, M. Verdult, M. Dijkstra, and R. van Roij, J. Chem. Phys. **135**, 134105 (2011).
[40]B. W. Kwaadgras, M. Dijkstra, and R. van Roij, J. Chem. Phys. **136**, 131102 (2012).
[41]Y. V. Shtogun and L. M. Woods, J. Phys. Chem. Lett. **1**, 1356 (2010).
[42]M. A. van der Hoef and P. A. Madden, J. Phys.: Condens. Matter **8**, 9669 (1996).